Tribo-dynamics of differential hypoid gears

Conference Paper · August 2013

DOI: 10.1533/9781782421955.340

3 authors:

Mahdi Mohammadpour
Loughborough University
106 PUBLICATIONS **766** CITATIONS
SEE PROFILE

Stephanos Theodossiades
Loughborough University
167 PUBLICATIONS **2,340** CITATIONS
SEE PROFILE

Homer Rahnejat
University of Central Lancashire
448 PUBLICATIONS **6,641** CITATIONS
SEE PROFILE

Proceedings of the ASME 2013 International Design Engineering Technical Conferences &
Computers and Information in Engineering Conference
IDETC/CIE 2013
August 4-7, 2013, Portland, Oregon, USA

DETC2013-12890

DRAFT: TRIBO-DYNAMICS OF DIFFERENTIAL HYPOID GEARS

Mahdi Mohammadpour
Wolfson School of Mechanical and Manufacturing Engineering
Loughborough University
Loughborough, UK
Email: M.Mohammad-Pour@lboro.ac.uk

Stephanos Theodossiades
Wolfson School of Mechanical and Manufacturing Engineering
Loughborough University
Loughborough, UK
Email: S.Theodossiades@lboro.ac.uk

Homer Rahnejat
Wolfson School of Mechanical and Manufacturing Engineering
Loughborough University
Loughborough, UK
Email: H.Rahnejat@lboro.ac.uk

ABSTRACT

Differential hypoid gears play an important role on the Noise, Vibration and Harshness (NVH) signature of vehicles. Additionally, the friction developed between their teeth flanks under extreme loading conditions adds another source of power loss in a drivetrain that absorbs vibrational energy. This work considers the coupling between dynamics and analytical tribology for the study of the dynamic response of hypoid gear pairs with lateral motion effects under a single framework. Elastohydrodynamic lubrication of point contact (EHL) has been assumed with Non-Newtonian, thermal and surface roughness effects in order to take in to account the effect of flank friction. Tooth Contact Analysis (TCA) has been used to obtain the input data required for the investigation. The dynamic behaviour and efficiency of a differential hypoid gear pair under realistic operating conditions are determined. The proposed tribo-dynamic framework provides a useful platform to conduct an extensive series of parametric studies.

NOMENCLATURE

a : Vehicle acceleration
b : Half amount of backlash
e : Static unloaded transmission error
G^* :Dimensionless material parameter
f_r : Total flank friction
f_b : Boundary friction contribution
f_v : Viscous friction contribution
h^*_{c0} : Dimensionless central film thickness
I_p : Moment of inertia of the pinion
I_g : Moment of inertia of the gear
k_{px} : Pinion bearing stiffness in x direction
k_{py} : Pinion bearing stiffness in y direction
k_{pz} : Pinion bearing stiffness in z direction
k_{gx} : Gear bearing stiffness in x direction
k_{gy} : Gear bearing stiffness in y direction
k_{gz} : Gear bearing stiffness in z direction
c_{px} : Pinion bearing damping in x direction
c_{py} : Pinion bearing damping in y direction
c_{pz} : Pinion bearing damping in z direction
c_{gx} : Gear bearing damping in x direction
c_{gy} : Gear bearing damping in y direction
c_{gz} : Gear bearing damping in z direction
m_p : Mass of the pinion
m_g : Mass of the gear
M : Vehicle mass
R_p , R_g : Pinion and gear contact radii
R_e , R_s : Dimensionless geometrical parameters
R_a : Aerodynamic resistance
R_{rl} : Rolling resistance
R_G : Gravitational resistance
r_t : Dynamic tire radius
T_p , T_g : Externally applied torque to the pinion and gear
T_{frp} , T_{frg} : Frictional moments at pinion and gear
U^* :Dimensionless speed parameter

W : Vehicle weight
W^* :Dimensionless load parameter
x_p : Pinion lateral displacement in x direction
y_p : Pinion lateral displacement in y direction
z_p : Pinion lateral displacement in z direction
x_g : Gear lateral displacement in x direction
y_g : Gear lateral displacement in y direction
z_g : Gear lateral displacement in z direction
μ : Coefficient of friction

Subscripts:

b : Denotes boundary contribution
g : Denotes the gear wheel
j : Refers to a teeth pair in mesh
p : Denotes the pinion
v : Refers to viscous shear

INTRODUCTION

Differential hypoid gears, being the final components in automotive drivetrains, are usually subjected to extreme loading conditions. The above fact underlines the important role of these elements on NVH, efficiency and lifetime in powertrains. Accurate dynamic models are essential to investigate the above research topics. In addition, a strong relationship between the dynamics and tribological behaviour is established through friction in the areas of contact of the interacting elements. Friction is the main source of power loss, also consuming some of the engine order energy input, which is responsible for a variety of NVH phenomena (rattle, whine, boom etc.). Thus, friction consumes energy, hence improving upon the lightly damped nature of the powertrain.

Due to the significance of gear mechanisms in engineering applications, the dynamics of gear pairs have been excessively studied. A number of works were dedicated on the dynamics of parallel axis transmissions [1-3] presented an analysis of such systems. However, limited investigations can be found on the dynamics of non-parallel axis gears, such as hypoid and bevel gears because of the complexity of gear kinematics and meshing characteristics. The mass-elastic model of rear axle gears with infinite mesh stiffness was studied in [4] to predict the pinion resonance and experiments were carried out to confirm the vibration peaks. A two degree-of-freedom (dof) vibration model of a pair of bevel gears was defined in [5], in which the line-of-action vector was modeled by a sine curve, to conduct stability analysis. In [6] it was experimentally found that axle gear noise could be reduced by modifying the vibration mode with the addition of an inertia disk that can be mounted on either side of the flanges of the final drive. An experimental method was proposed in [7] to study the body and driveline sensitivity to the transmission error of an axle hypoid gear pair. They calculated the force at the contact points of the gear teeth, and it was found that the dynamic mesh force was affected by the torsional vibration characteristics of the driveline. A dynamic model of a hypoid gear set was developed in [8] for use in finite element analysis of gearing systems, where the mesh point and line-of-action were time invariant. More recently, hypoid gear kinematic models based on the exact teeth geometry were proposed [9-11] to study the gear pair dynamics with transmission error excitation and Non-Linear Time Variant (NLTV) mesh characteristics. In another work [12], a NLTV dynamic model of a hypoid gear pair with mesh parameters described in a perfect sinusoidal form, was used to investigate the system response. A multipoint mesh model was developed in [13] and it was applied to analyze the hypoid gear dynamics. In all the above investigations, the time-dependent teeth mesh parameters have been expressed in the form of either fundamental harmonics or by considering a few harmonic orders. A dynamic model considering time varying contact parameters was developed in [14]. Recently a multi-body model for differentials considering component flexibility was presented in [15].

The mechanical inefficiencies in gearing arising from the EHL of meshing gear pairs, where a line contact approximation is made with flow along the contact width, have been investigated in [16-17]. Other researchers have used the more realistic assumption of elliptical point contact in hypoid gears [18-23]. A thermo-elastohydrodynamic analysis of hypoid gear pairs with point contact geometry was presented in [24]. Nevertheless, the input torque was relatively low and not representative of vehicle differentials. Again, the flow vector was assumed to be along the minor axis of the contact ellipse. However, experimental evidence [25] and numerical investigations [26-28] have suggested significant side-leakage flow along the major axis of the contact ellipse. The repercussion is that continuity of flow would be breached, as well as errors are introduced in the evaluation of contact temperatures due to side leakage flow. The assumption of a line contact footprint can be considered as reasonable in conditions that promote an elliptical point contact of large aspect ratio. In [16-17] and [24], EHL was applied on gear meshing problems through TCA, where for the completeness of the solution elliptical contact conditions were assumed at relatively low contact loads. Recently, in [29] TCA was applied in the EHL calculations of a hypoid gear pair with angled flow and point contact assumptions. However, this work doesn't take into consideration the dynamic behaviour of the gear pair. In [30], a dynamic investigation coupled with tribology has been conducted for differential hypoid gears. The torsional motions of the gear wheels (two-degree of freedom model) have been considered.

This paper presents a numerical model of differential hypoid gears, considering the lateral motion of their shafts, as well as the torsional motions of the gear wheels. Due to the geometrical complexity of the interacting teeth surfaces, TCA was used to obtain the required gear input data (CALYX software). These include the varying geometry of contact and teeth meshing stiffness. The stiffness of the supporting bearings

is also considered to be nonlinear. Dynamics and analytical tribology are coupled in the model (tribo-dynamics), in order to include the effect of lubrication. Due to the high loads transferred at the engaged flanks, EHL point contact is assumed with Non-Newtonian, thermal and surface roughness effects. The data exchange between dynamics and tribology provides the dynamic model with the information on friction whereas the instantaneous contact load is fed to the tribology routine to establish the bi-directional interactions. An iterative process is required to complete the methodology.

MODEL DESCRIPTION

The multi-body model of the hypoid gear pair is eight degrees of freedom and it has been developed in the commercial software ADAMS (Fig. 1). Degrees of freedom include lateral motions of shafts as well as torsional motions. The inertial properties of the mating gear pair are listed in Table 1. The model can be reduced to seven degrees of freedom, eliminating the rigid body torsional mode. The procedure is presented in [31].

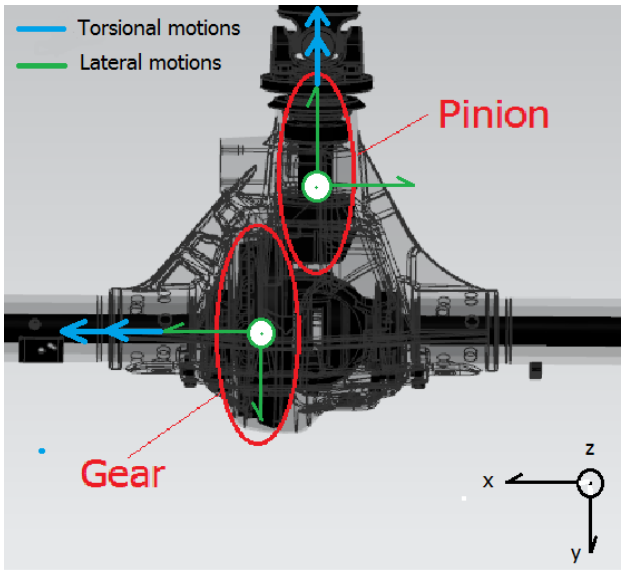

Figure 1. AN OVERVIEW OF THE MULTI-BODY DYNAMICS MODEL

Table 1. INERTIA PROPERTIES AND MASS

Part number	Part name	Inertia [kg m2]	Mass [kg]
1	Ground	-----	-----
2	Pinion	$1734 \cdot 10^{-6}$	12
3	Gear	$5.81 \cdot 10^{-2}$	49.9

This seven-degree of freedom model can be presented in the set of Eqn.1

$$[M]\ddot{X} + [C]\dot{X} + [K]X = F \tag{1}$$

where

$$[M] = \begin{bmatrix} m & -n_x m & -n_y m & -n_z m & n_x m & n_y m & n_z m \\ -n_x m & m_p + {n_x}^2 m & n_y n_x m & n_z n_x m & -n_x n_x m & -n_y n_x m & -n_z n_x m \\ -n_y m & n_x n_y m & m_p + {n_y}^2 m & n_z n_y m & -n_x n_y m & -n_y n_y m & -n_z n_y m \\ -n_z m & n_x n_z m & n_y n_z m & m_p + {n_z}^2 m & -n_x n_z m & -n_y n_z m & -n_z n_z m \\ n_x m & -n_x n_x m & -n_y n_x m & -n_z n_x m & m_g + {n_x}^2 m & n_y n_x m & n_z n_x m \\ n_y m & -n_x n_y m & -n_y n_y m & -n_z n_y m & n_x n_y m & m_g + {n_y}^2 m & n_z n_y m \\ n_z m & -n_x n_z m & -n_y n_z m & -n_z n_z m & n_x n_z m & n_y n_z m & m_g + {n_z}^2 m \end{bmatrix}$$

$$[C] = \begin{bmatrix} c_m & 0 & 0 & 0 & 0 & 0 & 0 \\ 0 & c_{px} & 0 & 0 & 0 & 0 & 0 \\ 0 & 0 & c_{py} & 0 & 0 & 0 & 0 \\ 0 & 0 & 0 & c_{pz} & 0 & 0 & 0 \\ 0 & 0 & 0 & 0 & c_{gx} & 0 & 0 \\ 0 & 0 & 0 & 0 & 0 & c_{gy} & 0 \\ 0 & 0 & 0 & 0 & 0 & 0 & c_{gz} \end{bmatrix}$$

$$[K] = \begin{bmatrix} k_m & 0 & 0 & 0 & 0 & 0 & 0 \\ 0 & k_{px} & 0 & 0 & 0 & 0 & 0 \\ 0 & 0 & k_{py} & 0 & 0 & 0 & 0 \\ 0 & 0 & 0 & k_{pz} & 0 & 0 & 0 \\ 0 & 0 & 0 & 0 & k_{gx} & 0 & 0 \\ 0 & 0 & 0 & 0 & 0 & k_{gy} & 0 \\ 0 & 0 & 0 & 0 & 0 & 0 & k_{gz} \end{bmatrix}$$

$$[X] = \begin{bmatrix} x \\ x_{px} \\ x_{py} \\ x_{pz} \\ x_{px} \\ x_{py} \\ x_{pz} \end{bmatrix}, \quad [F] = \begin{bmatrix} F \\ n_x F \\ n_y F \\ n_z F \\ -n_x F \\ -n_y F \\ -n_z F \end{bmatrix}$$

where k_m is the meshing stiffness obtained by TCA, which is provided to the system as a Fourier series [32], c_m is the structural torsional damping coefficient and m is the equivalent mass in the direction of the line of action. It is defined as:

$$m = \frac{I_p I_g}{I_p R_g^2 + I_g R_p^2} \tag{2}$$

F is defined as:

$$F = m\left[\frac{R_p T_p}{I_p} + \frac{R_g T_g}{I_g} - \ddot{e}(t)\right] \tag{3}$$

$f(x)$ is defined as follows, in order to take into account the effect of backlash:

$$f(x) = \begin{cases} x - b, & x \geq b \\ 0, & -b < x < b \\ x + b, & x \leq -b \end{cases} \tag{4}$$

where x denotes the instantaneous line of approach between engaged teeth pairs. This is the Dynamic Transmission Error (DTE), hence:

$$x(t) = \int_0^t R_p \dot{\psi}_p dt - \int_0^t R_g \dot{\psi}_g dt - U_g + U_p - e(t) \tag{5}$$

where

$$U_g - U_p = \left(+n_x x_{gx} + n_y x_{gy} + n_z x_{gz} - n_x x_{px} - n_y x_{py} - n_z x_{pz}\right) \quad (6)$$

is the relative displacement between the pinion and gear in the direction of the instantaneous line of action. This is obtained using the components of instantaneous unit vectors in the direction of the line of action (n_x ,n_y ,n_z). The unit vectors are obtained from TCA and are employed in the form of Fourier series.

In order to determine the coefficients of damping and natural frequencies, the method described in [33] has been used. The damping ratio has been assumed as 3% in the torsional direction and 2% in the lateral directions, according to [10].
The applied forces T_i in the torsional directions are the torques on the pinion and gear, as well as the contribution due to flank friction:

$$T_i = T_{ai} + T_{fri} \quad (7)$$

The stiffness of bearings is calculated considering non-linearity of these components based on presented procedure in [34]. This model presents the stiffness reaction force instantaneously considering the applied torque.

THE RESISTING TORQUE ON THE WHEEL

The torque applied to the wheels includes the vehicle inertia effect, rolling friction resistance, aerodynamic resisting force and grading load [35]:

$$T_{ag} = r_t \sum F \quad (8)$$

where r_t is the dynamic tire radius and $\sum F$ is obtained from vehicle longitudinal dynamics as:

$$\sum F = ma = R_a + R_{rl} + R_G \quad (9)$$

The instantaneous input torque, T_{ap}, from the engine (on the pinion) is defined using the same approach in [32].

THE FLANK FRICTION

The friction of flank between the engaged pair of gear teeth contributes to the excitation of the system. A thin elastohydrodynamic lubricant film is assumed between the meshing teeth pairs, which is subject to non-Newtonian viscous shear, supplemented by any asperity interactions (boundary friction as the result of the direct contact of surfaces) and angled flow. Therefore, it is:

$$T_{fri} = R_i f_r \quad (10)$$

where the flank friction is given by

$$f_r = f_v + f_b \quad (11)$$

The viscous friction is given by

$$f_r = \mu F_i \quad (12)$$

An analytical-experimental equation for the calculation of the friction coefficient is presented in [36], considering the non-Newtonian behaviour of the lubricant and thermal effects. The same method has been used in this work.

To calculate boundary friction, the presented method in [37] is used. This model assumes Gaussian distribution of the asperity heights, with a mean radius of curvature for an asperity summit. A full procedure of this method has been provided in [29].

The film thickness h is required for friction calculations that can be obtained using an extrapolated expression [26-27] for elliptical point contacts with angled lubricant flow entrainment in the conjunction:

$$h_{c0}^* = 4.31 U^{*0.68} G^{*.49} W^{*-0.073} \left\{1 - exp\left[-1.23\left(\frac{R_s}{R_e}\right)^{2/3}\right]\right\} \quad (13)$$

where, the non-dimensional groups are described in [26-27].

TOOTH CONTACT ANALYSIS (TCA)

It is necessary to calculate the contact load F_i for all the simultaneous meshing teeth pairs, which is required for both complete models. This is obtained from TCA. The method is described in detail in [38]. Data for obtained from TCA include the instantaneous contact radii of curvature of the teeth surfaces, the contact stiffness and the static transmission error. The contact load per teeth pair is a function of the dynamic response. However, its distribution among teeth pairs in simultaneous contact can be defined quasi-statically. A load distribution factor is calculated as a function of the pinion angle for all teeth contacts. This is the ratio of the applied load F_i on a given flank under consideration to the total transmitted load F_t [16]:

$$lf = \frac{F_i}{F_t} \quad (14)$$

Details regarding the face hobbed, lapped hypoid gear pair used in this study are provided in [29].

RESULTS AND DISCUSSION

The current analysis investigates the NVH behavior for a pair of differential hypoid gears of a light truck. The related

input parameters and physical properties needed for the analysis are presented in Tab. 2 and 3.

Table 2. INPUT OPERATING CONDITIONS

Parameter name	**Value**
Frontal area	2.2 m^2
Coefficient of rolling resistance	0.0166
Drag coefficient	0.33
Air density	1.22 kg/m^3
Vehicle weight	1300 kg
Tyre (type)	P205/65R15 BSW
Gear ratio	0.951:1
Surface roughness of solids	0.5 μm

Table 3. PHYSICAL PROPERTIES OF THE LUBRICANT AND SOLIDS

Pressure viscosity coefficient (α)	2.383x10-8[Pa^{-1}]
Lubricant dynamic viscosity at 100°C	0.0171[Pa.s]
Heat capacity of fluid	0.14 [J/kg˚K]
Thermal conductivity of fluid	2000 [W/m˚K]
Modulus of elasticity of contacting solids	210 [GPa]
Poisson's ratio of contacting solids	0.3 [-]
Density of contacting solids	7850[kg/m^3]
Thermal conductivity of contacting solids	46 [W/m˚K]
Heat capacity of contacting solids	470 [J/kg˚K]

Most of the critical phenomena in relation to efficiency and NVH usually take place during transient conditions (acceleration and deceleration). In this work, simulation of accelerating driving conditions is presented. The torque is assumed to be rising from 98 N.m to 145 N.m within 0.5 s, and then the system remains constant in this torque for more than 10 seconds. Figure 2 shows the calculated vehicle speed during this simulation. Results are presented in three categories:

1. Complete model considering non-linear bearing stiffness.
2. Torsional model only (neglecting lateral DOFs).
3. Complete model considering higher non-linear bearing stiffness than that of category 1.

In all the above simulations, the DTE, lateral motions and force transmissibility through the bearings. For DTE and lateral displacement calculations, the peak to peak value is important in terms of potential noise generation. In addition, teeth separation is another source of vibration severity. The force transmissibility is important for the prediction of excitation conditions that lead the differential housing (structural borne noise generation).

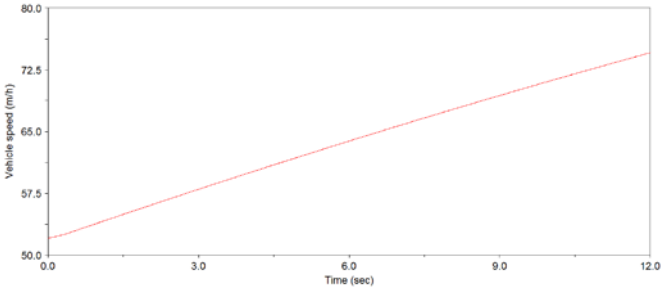

Figure 2. VEHICLE SPEED TIME HISTORY

Torsional-lateral model with non-linear bearings

The DTE time history is presented in Fig. 3. The maximum peak to peak value is between 80-120 μm. Moreover, the teeth flanks are always in contact. Fig. 4 presents the corresponding wavelet plot, which shows that the dominant frequencies are engine orders and meshing frequencies. The energy carried by the first meshing frequency varies, although it is dominant for a considerable part of the spectrum.

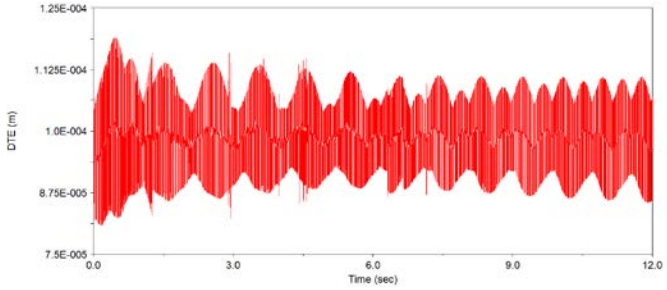

Figure 3. DTE TIME HISTORY OF THE COMPLETE MODEL WITH NONLINEAR BEARINGS

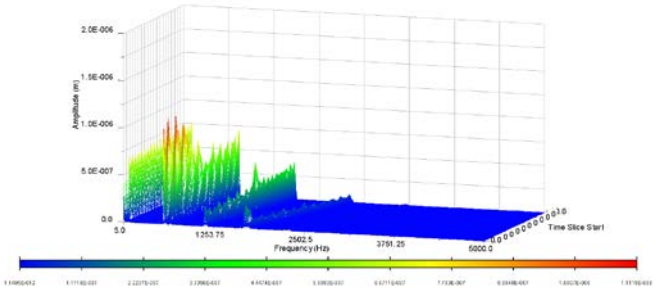

Figure 4. WAVELET PLOT OF THE DTE TIME HISTORY OF FIG. 3

Figure 5 exhibits the transmitted lateral force through the supporting bearing elements. This is calculated using the following equation.

$$F = x_g k_g + \dot{x_g} c_g \quad (15)$$

This parameter is important, since it influences the structural vibration characteristics of the transfer path between the hypoid gears and the vehicle chassis. In the case of differentials, the

main NVH issue is axle whine, which is a structural borne noise phenomenon. The corresponding wavelet of Fig. 6 shows that the frequency content of the excitation force on bearings is characterized by the meshing frequency orders, whereas the engine orders have less contribution. This is in contrast with the observations from the DTE wavelet of Fig. 3. In addition, the intensity of each meshing frequency order varies with the vehicle speed.

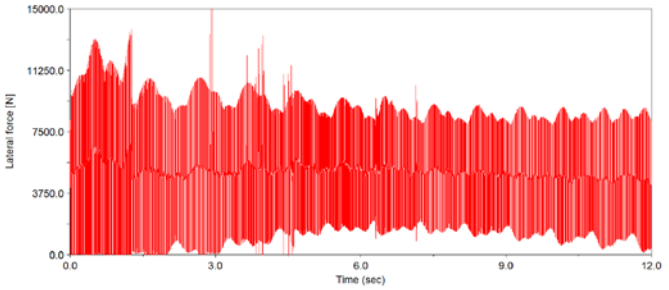

Figure 5. TRANSMITTED LATERAL FORCE - COMPLETE MODEL WITH NONLINEAR BEARINGS

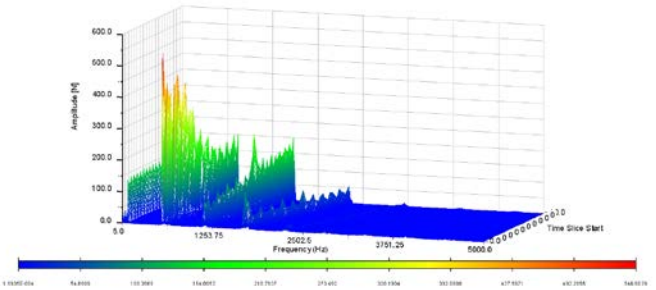

Figure 6. WAVELET THE TRANSMITTED LATERAL FORCE OF FIG. 5

Model with torsional degrees of freedom only

Results are presented from a model with torsional degrees of freedom only (rotation of the gear wheels). The DTE time history presented in Fig. 7 shows higher peak to peak values compared to the complete model (Fig. 3), exaggerating its NVH performance. This is expected, since the energy carried cannot ease in more directions than the two rotations employed in this simplified model. The corresponding wavelet of Fig. 8 shows again contributions of the engine and meshing frequency orders. However, the trend this time – in contrast to the wavelet of the complete model in Fig. 4 – is for the first meshing frequency to dominate as the speed of the vehicle increases, which can be misleading.

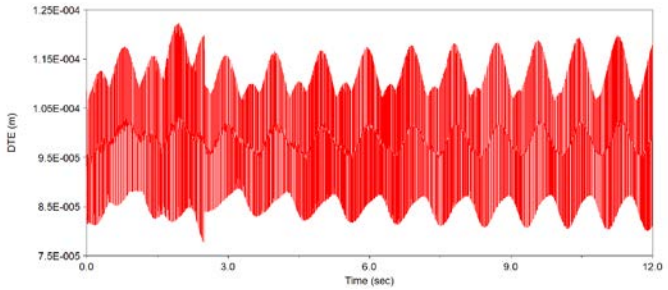

Figure 7. DTE TIME HISTORY OF THE MODEL WITH TORSIONAL DEGREES OF FREEDOM ONLY

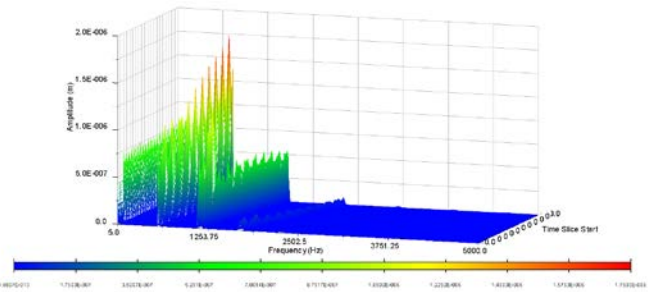

Figure 8. WAVELET PLOT OF THE DTE TIME HISTORY OF FIG. 7

Torsional-lateral model with non-linear bearings of higher stiffness

The DTE time history of the complete model equipped with nonlinear bearings of higher stiffness is presented in Fig. 9, whereas the corresponding wavelet plot is shown in Fig. 10. It can be seen that higher stiffness values lead to higher peak to peak DTE amplitudes that increase, as the vehicle speed increases. The wavelet frequency content follows that of the torsional model (Fig. 7) to a large extent rather than that of the complete model with lower bearing stiffness (Fig. 4), since the meshing frequency orders are dominating in Fig. 10 with increasing vehicle speed.

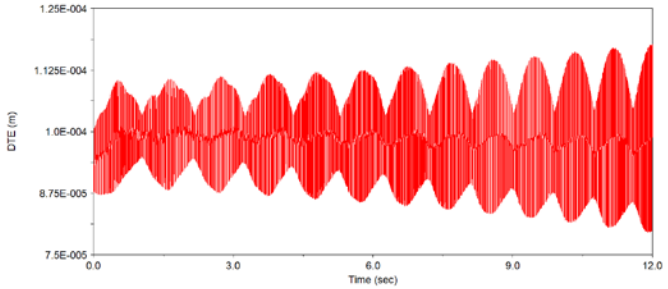

Figure 9. DTE TIME HISTORY OF THE COMPLETE MODEL WITH NONLINEAR BEARINGS (HIGHER STIFFNESS)

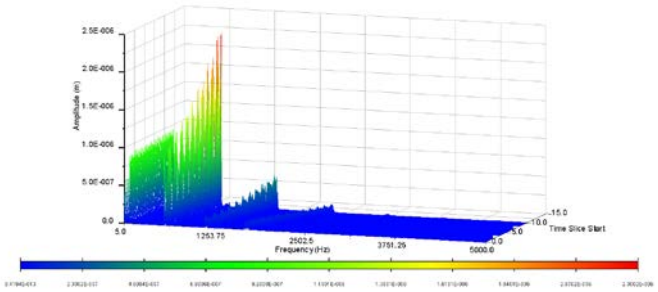

Figure 10. WAVELET PLOT OF THE DTE TIME HISTORY OF FIG. 9

Figure 11 shows the transmitted force time history, as it has been calculated in the *x* direction of the gear. Fig. 12 is the corresponding wavelet. As it can be seen, higher bearing stiffness incurs higher loads transferred to the housing, thus worsening the NVH performance. The wavelet shows clear domination of the first meshing frequency throughout the vehicle speed range.

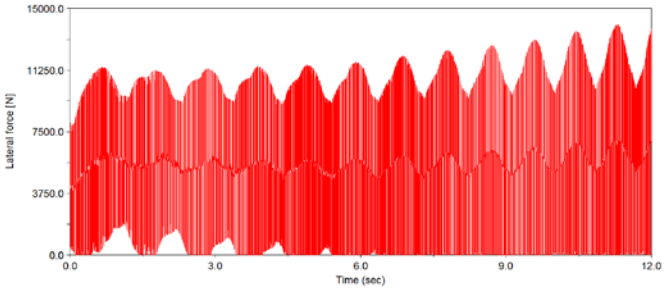

Figure 11. TRANSMITTED LATERAL FORCE - COMPLETE MODEL WITH NONLINEAR BEARINGS (HIGHER STIFFNESS)

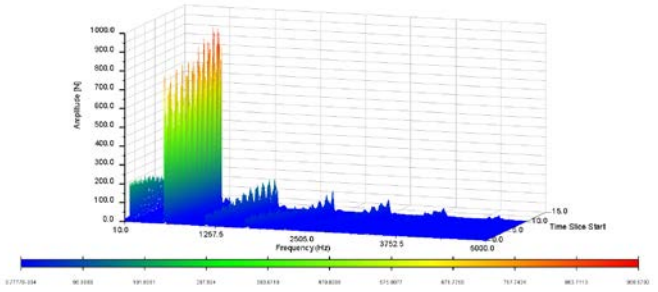

Figure 12. WAVELET THE TRANSMITTED LATERAL FORCE OF FIG. 11 (HIGHER STIFFNESS)

CONCLUDING REMARKS

Efficiency and NVH are two main concerns of hypoid gear pairs. These two performance indices can be estimated at an early design stage using numerical models that follow a tribo-dynamic approach. In the tribological aspect of this work, elastohydrodynamic point contacts with angled flow are assumed between the teeth flanks. TCA provides the necessary geometric and kinematic data while the dynamics yield the applied loads. On the dynamics side, a torsional/lateral model of the gear pairs is employed, where the nonlinearity of meshing and bearing stiffness is taken into account. The force transmissibility through the bearings is calculated, which is a key point for axle whine investigations. These preliminary results indicate that higher bearing stiffness leads to worse NVH performance.

REFERENCES

[1] Ozguven, H. N. Houser, D. R. ‘mathematical models used in gear dynamics- A review’, Journal of Sound and Vibration 121 (3), 383-411 (1988)

[2] Kahraman A. Singh, R. ‘interactions between the time varying mesh stiffness and clearance nonlinearities in a geared system’, Journal of Sound and Vibration 146 (1), 135-156, (1991)

[3] Amabili, M. Rivola, A. ‘Dynamic analysis of spur gear pairs: steady-state response and stability of the SDOF model with time varying mesh damping’, Mechanical Systems and Signal Processing 11, 375–390, (1997)

[4] E.P. Remmers, Dynamics of automotive rear axle gear noise. SAE Paper 710114, (1971)

[5] Kiyono, S. Fujii, Y. Suzuki, Y. ‘Analysis of vibration of bevel gears’, Bulletin of the Japan Society of Mechanical Engineers 24, 441–446, (1981)

[6] Abe, E. Hagiwara, H. ‘Advanced Method for Reduction in Axle Gear Noise’, Gear Design, Manufacturing and Inspection Manual, Society of Automotive Engineers, 223–236, (1990)

[7] Hirasaka, N. Sugita, H. Asai, M. ‘A simulation method of rear axle gear noise’, Journal of Passenger Cars 100, 1383–1387, (1991)

[8] Donley, M.G. Lim, T.C. Steyer, G.C. ‘Dynamic analysis of automotive gearing systems’, Journal of Passenger Cars 101, 77 87, (1992)

[9] Cheng, Y. Lim, T.C. ‘Dynamic analysis of high speed hypoid gears with emphasis on automotive axle noise problem’, Proceedings of the ASME Power Transmission and Gearing Conference, DETC98/PTG-5784, Atlanta, GA, (1998)

[10] Cheng, Y. Lim, T.C. ‘Dynamics of hypoid gear transmission with time-varying mesh’, Proceedings of the ASME Power Transmission and Gearing Conference, DETC2000/PTG-14432, Baltimore, MD, (2000)

[11] Cheng, Y. Lim, T.C. ‘Vibration analysis of hypoid transmissions applying an exact geometry-based gear mesh theory’, Journal of Sound and Vibration 240, 519–543, (2001)

[12] Jiang, X. ‘Non-linear Torsional Dynamic Analysis of Hypoid Gear Pairs’, MSc Thesis, The University of Alabama, (2002)

[13] Wang, H. ‘Gear Mesh Characteristics and Dynamics of Hypoid Geared Rotor System’, PhD Dissertation. The University of Alabama, (2002)

[14] Wang, J. Lim, T. C. Li, M. 'Dynamics of a hypoid gear pair considering the effects of time-varying mesh parameters and backlash nonlinearity', Journal of Sound and Vibration, 229 (2), 287-310, (2007)
[15] Virlez, G. Bruls, O. Duysinx, P. and Poulet, N. "simulation of differentials in four-wheel drive vehicles using multi-body dynamics", ASME, DETC2011. (2011)
[16] Xu, H. and Kahraman, A. "Prediction of friction-related power losses of hypoid gear pairs", Proc. Instn. Mech. Engrs, J. Multi-body Dyn., 221, 387-400 (2007)
[17] Kolivand, M., Li, S. and Kahraman, A. "Prediction of mechanical gear mesh efficiency of hypoid gear pairs", Mech. & Mach. Theory, 45, 1568–1582 (2010)
[18] Sidle, R. W., Archard, J. F., "LUBRICATION AT ELLIPTICAL CONTACTS", Proc Instn Mech Engrr, 183, 138-146 (1968-69)
[19] Simon, V., "The influence of misalignments on mesh performances of hypoid gears", Mechanism and Machine Theory, 33, 1277-1291 (1998)
[20] Simon, V., "Influence of Machine Tool Setting Parameters on EHD Lubrication in Hypoid Gears", 12th IFToMM World Congress, Besançon (France), June18-21, (2007)
[21] Simon, V., "Load Distribution in Hypoid Gears", ASME, Journal of Mechanical Design, 122, 529-535, (2000)
[22] Simon, V., "FEM stress analysis in hypoid gears", Mechanism and Machine Theory, 35, 1197-1220 (2000)
[23] Ito, N., Takahashi, K., "Differential Geometrical Conditions of Hypoid Gears with Conjugate Tooth Surfaces", ASME, Journal of Mechanical Design, 122, 323-330, (2000)
[24] Simon, V. "Influence of machine tool setting parameters on EHD lubrication in hypoid gears", Mech. & Mach. Theory, 44, 923–937 (2009)
[25] Gohar, R. "Oil film thickness and rolling friction in elastohydrodynamic point contact", Trans. ASME, J. Lubn. Tech., 93, (1971)
[26] Chittenden, R. J., Dowson, D., Dunn, J. F. and Taylor, C. M. "A theoretical analysis of the isothermal elastohydrodynamic lubrication of concentrated contacts. I. Direction of lubricant entrainment coincident with the major axis of the Hertzian contact ellipse", Proc. Roy. Soc., Ser. A, 397, 245-269 (1985)
[27] Chittenden, R. J., Dowson, D., Dunn, J. F. and Taylor, C. M. "A theoretical analysis of the isothermal elastohydrodynamic lubrication of concentrated contacts. II. General Case, with lubricant entrainment along either principal axis of the Hertzian contact ellipse or at some intermediate angle", Proc. Roy. Soc., Ser. A, 397, 271-294 (1985).
[28] Jalali-Vahid, D., Rahnejat, H., Gohar, R. and Jin, Z.M "Prediction of oil-film thickness and shape in elliptical point contacts under combined rolling and sliding motion", Proc. Instn. Mech. Engrs., J. Engng. Trib., 214, 427-437 (2000)
[29] Mohammadpour, M., Theodossiades, S. and Rahnejat, H. "Elastohydrodynamic lubrication of hypoid gears at high loads", Proc. Instn. Mech. Engrs., Part J: J. Engng. Tribology, 2012, 226 (3), pp. 183-198
[30] Mohammadpour, M., Theodossiades, S., Rahnejat, H. and Kelly, P. "Transmission efficiency and NVH refinement of differential hypoid gear pairs", Submitted to the Proc. Instn. Mech. Engrs., Part K: J. Multi-Body Dynamics.
[31] Theodossiades, S. and Natsiavas, S. "On geared rotordynamic systems with oil journal bearings", Journal of sound and vibration, 2001, 243 (4), pp. 721-745.
[32] Karagiannis, Y., Theodossiades, S. and Rahnejat, H. "On the dynamics of lubricated hypoid gears", Mechanism & and Machine Theory, 2012, 48, pp. 94-120
[33] Caughey, T. K. "Classical normal modes in damped linear dynamic systems", Journal of Applied Mechanics, 1960, 27, p 269-271
[34] Harris, T. and Kotzalas, M. N., Advanced Concepts of Bearing Technology, Taylors and Francis, 2007
[35] Gillespie, T. D. Fundamentals of Vehicle Dynamics, Society of Automotive Engineering, Inc. Pa, USA, 1992
[36] Evans, C. R. and Johnson, K. L. "Regimes of traction in elastohydrodynamic lubrication", Proc. Instn. Mech. Engrs., 1986, 200 (C5), pp. 313–324
[37] Greenwood, J. A. and Tripp, J. H. "The contact of two nominally flat rough surfaces", Proc. Instn. Mech. Engrs, 1970-71. 185, pp. 625-633
[38] Litvin, F. L. and Fuentes, A. Gear Geometry and Applied Theory, 2nd ed., Cambridge University Press, New York, 2004